

# Lawrence Berkeley National Laboratory

## LBL Publications

### Title

Band anticrossing in Group II-Ox-VI<sub>1-x</sub> highly mismatched alloys: Cd<sub>1-y</sub>MnyOxTe<sub>1-x</sub> quaternaries synthesized by O ion implantation

### Permalink

<https://escholarship.org/uc/item/0167w6qz>

### Journal

Applied Physics Letters, 80(9)

### Author

Becla, P.

### Publication Date

2001-11-05

***Band Anticrossing in Group II-O<sub>x</sub>-VI<sub>1-x</sub> Highly Mismatched Alloys:  
Cd<sub>1-y</sub>Mn<sub>y</sub>O<sub>x</sub>Te<sub>1-x</sub> Quaternaries Synthesized by O Ion Implantation***

K. M. Yu, W. Walukiewicz, J. Wu, J. W. Beeman, J. W. Ager III, E. E. Haller,  
Materials Sciences Division, Lawrence Berkeley National Laboratory,  
Berkeley, California 94720

I. Miotkowski, and A. K. Ramdas

Department of Physics, Purdue University, West Lafayette, Indiana 47907

P. Becla

Department of Materials Science and Engineering, Massachusetts Institute of  
Technology, Cambridge, Massachusetts 02139

ABSTRACT

Highly mismatched group II-O<sub>x</sub>-VI<sub>1-x</sub> alloys have been synthesized by oxygen implantation into Cd<sub>1-y</sub>Mn<sub>y</sub>Te crystals. In crystals with  $y > 0.02$ , incorporation of O causes a large decrease in the band gap. The band gap reduction increases with  $y$ ; the largest value observed is 190 meV in O-implanted Cd<sub>0.38</sub>Mn<sub>0.62</sub>Te. This striking behavior is consistent with the band anticrossing (BAC) model which predicts that a repulsive interaction between localized states of O located above the conduction band edge and the extended states of the conduction band causes the band gap reduction. These large, O-induced effects provide a unique opportunity to control band gaps, conduction band offsets, and electronic properties in this new class of group II-O<sub>x</sub>-VI<sub>1-x</sub> alloys.

*PACS numbers: 78.66.Hf; 78.20.-e; 61.72.Vv; 81.05.Dz*

Compound semiconductor alloys in which the anions are partially replaced by isoelectronic atoms, with distinctly larger electronegativity have recently attracted significant attention. Group III-N<sub>x</sub>-V<sub>1-x</sub> alloys (e.g. GaN<sub>x</sub>As<sub>1-x</sub>) in which a small amount (up to ~5%) of the electronegative N substitutes the more metallic column V element, have been the most extensively studied class of such Highly Mismatched Alloys (HMAs) [1-7]. The most striking feature of these III-N<sub>x</sub>-V<sub>1-x</sub> alloys is the large N-induced reduction of the band gap (>100meV for  $x \sim 0.01$ ).

It has been shown recently that the unusual properties of the III-N<sub>x</sub>-V<sub>1-x</sub> alloys can be well explained by the band anticrossing (BAC) model [8, 9]. In this model a repulsive interaction between the localized nitrogen states, which are located above the conduction band edge, and the extended states of the host semiconductor matrix splits the conduction band of the matrix semiconductor into two subbands. The downward shift of the lower subband is responsible for the large reduction of the fundamental gap. Moreover, the BAC model also predicts a considerable flattening of the lower subband near its minimum, resulting in a large increase of the electron effective mass [9, 10]. Recently, the BAC model has also been applied to the II-VI ternary alloys, ZnS<sub>x</sub>Te<sub>1-x</sub> and ZnSe<sub>y</sub>Te<sub>1-y</sub>, in which replacing the more metallic Te atoms with the more electronegative S or Se leads to band gap reductions at small values of  $x$  and  $y$  [11].

Since the strength of the anticrossing interaction in HMAs depends on the electronegativity mismatch, one can anticipate it to be particularly pronounced in group II-O<sub>x</sub>-VI<sub>1-x</sub> alloys in view of the very highly electronegative O atoms substituting the significantly more metallic column VI elements [11]. The incorporation of the large concentration of oxygen, frequently present in II-VI compounds as an impurity, has proven to be technically challenging. In this Letter we demonstrate the successful formation of Cd<sub>1-y</sub>Mn<sub>y</sub>O<sub>x</sub>Te<sub>1-y</sub> alloys by O ion implantation in Cd<sub>1-y</sub>Mn<sub>y</sub>Te. In a remarkable agreement with the band anticrossing model, we indeed observe a strikingly strong O-induced reduction of the fundamental band gap. Our results demonstrate the

existence of a new class of HMAs in which the alloying effects are even more striking than in the more extensively studied III-N<sub>x</sub>-V<sub>1-x</sub> alloys.

Multiple energy (30, 80 and 160keV) O<sup>+</sup> implantation was carried out in single crystal Cd<sub>1-y</sub>Mn<sub>y</sub>Te (0<y<0.65) ternaries grown by vertical gradient freezing technique [12], forming ~0.3 μm thick Cd<sub>1-y</sub>Mn<sub>y</sub>O<sub>x</sub>Te<sub>1-y</sub> layers with relatively constant O concentrations of ~2.5x10<sup>20</sup> and ~5x10<sup>20</sup> cm<sup>-3</sup>. These correspond to implanted O mole fractions of 0.027 (low dose) and 0.054 (high dose), respectively. The implanted samples were subjected to rapid thermal annealing (RTA) for 10 s at temperatures ranging from 300 to 800°C to remove the implant damage and “activate” the implanted O atoms.

Band gaps of the synthesized alloys were measured using photomodulated reflectance (PR) spectroscopy at room temperature. Radiation from a 300W halogen tungsten lamp dispersed by a 0.5 m monochromator was focused on the samples as a probe beam. A chopped HeCd laser beam (λ=4420 Å) provided the photomodulation. PR signals were detected by a Si photodiode using a phase-sensitive lock-in amplification system. The values of the band gap and the line width broadening were determined by fitting the PR spectra to the Aspnes third-derivative functional form [13].

Figure 1 shows the PR spectra from three low dose (y=0.017, 0.043 and 0.19), a high dose (y=0.19) O-implanted Cd<sub>1-y</sub>Mn<sub>y</sub>Te samples after RTA at 600°C, and the corresponding as-grown Cd<sub>1-y</sub>Mn<sub>y</sub>Te crystals. Band gap reductions (ΔE) are immediately evident in the samples with y = 0.043 and 0.19. In contrast, in the sample with the lowest Mn content, y = 0.017, only a small band gap reduction of less than 10 meV is observed.

From Fig. 1 we clearly observe that Mn leads to increased stability of substitutional O in the case of Cd<sub>1-y</sub>Mn<sub>y</sub>Te. We believe that the presence of Mn enhances the incorporation of O on the Te sublattice, possibly due to the formation of relatively strong Mn-O bonds. For samples with a Mn mole fraction of 0.19 implanted with 2.7% of O, a ΔE as large as 60 meV, remaining stable up to an annealing temperature of 800°C, is observed. The dependence of ΔE on the implanted O dose can be seen in the PR spectra

of the high and low dose O implanted  $\text{Cd}_{0.81}\text{Mn}_{0.19}\text{Te}$  samples shown in figure 1 (top two spectra). A 25% increase in  $\Delta E$  (from 60meV to 75meV) is observed when the implanted O dose doubles.

PR measurements on as-grown  $\text{Cd}_{1-y}\text{Mn}_y\text{Te}$  samples subjected to annealing to 800°C showed no band gap shift. Several  $\text{Cd}_{1-y}\text{Mn}_y\text{Te}$  crystals with  $y=0$  and 0.2 were implanted with Ne and Cl to doses chosen to create implant damage profiles comparable to the low dose O-implanted samples [14]. These  $\text{Cd}_{1-y}\text{Mn}_y\text{Te}$  crystals with no implanted O did show a band gap reduction that was as large as 25 meV. However, at the temperatures used to activate the O-implanted samples, i.e.,  $T > 500^\circ\text{C}$ , this damage induced band gap reduction decreased to  $< 8\text{meV}$ . We therefore conclude that the observed band gap reductions in the O implanted samples are *not* caused by high temperature annealing or lattice damage.

According to the BAC model the dispersion relations for the upper and lower conduction subbands in HMAs are given by [8,9]

$$E_{\pm}(k) = \frac{1}{2} \left[ E_L + E_M(k) \pm \sqrt{(E_L - E_M(k))^2 + 4C_{LM}^2 x} \right] \quad (1)$$

where  $E_L$  is the energy of the localized level introduced by the more electronegative, isoelectronic atoms,  $E_M(k)$  is the dispersion relation for the conduction band of the host semiconductor matrix, and  $C_{LM}$  is the matrix element describing the coupling between localized states and the extended states. For  $\text{GaN}_x\text{As}_{1-x}$ , the downward shift of the lower subband  $E_-$  can account well for the reduction of the fundamental band gap using the known values of  $E_N=1.65$  eV above the VB maximum and  $C_{NM}=2.7$  eV [9]. In the case of II-V alloys a matrix element  $C_{LM}=1\text{eV}$  was measured in  $\text{ZnSe}_x\text{Te}_{1-x}$  and  $\text{ZnS}_y\text{Te}_{1-y}$  HMAs [11]. It is believed that the magnitude of this matrix element depends on the electronegativity difference between the matrix anion elements. In this work  $C_{OM}$  cannot

be determined independently because a precise measurement of the fraction of O on the Te sublattice (i.e.,  $x$ ) is not possible.

At doping concentrations, oxygen was known to form a localized level in the gap with an energy  $E_O = 2.0$  eV above the VB edge [15]. It has been shown previously that the energy of the oxygen level,  $E_O$  is constant in the absolute energy reference [11]. Therefore the composition dependence of  $E_O$  can be estimated from the known band offsets between ZnTe and CdTe with respect to the  $\text{Cd}_{1-y}\text{Mn}_y\text{Te}$  valence band edge as  $E_O = 1.9 + 0.59y$  (eV). This means that  $E_O$  is resonant with the conduction band in  $\text{Cd}_{1-y}\text{Mn}_y\text{Te}$  when  $0 < y < 0.5$ .

Using our estimated  $E_O$  in Eq. (1), the observed band gap reductions for the  $\text{Cd}_{0.81}\text{Mn}_{0.19}\text{Te}$  samples shown in Fig. 1 can be explained with  $C_{OM}^2 x$  values of 0.016 and 0.018 for implanted O contents of 2.7 and 5.4%, respectively. Since the electronegativity difference between O and Te is larger than that between N and As, we make a further assumption that  $C_{OM} \approx 3.5$  eV. With these assumptions, we estimate that the substitutional O content (i.e.,  $x$ ) in the  $\text{Cd}_{0.81}\text{Mn}_{0.19}\text{O}_x\text{Te}_{1-x}$  alloys formed by O-implantation in Fig. 1 to be  $\sim 0.0013$  and  $0.0024$  for the low and high dose samples. This corresponds to an “activation” efficiency (i.e., ratio of the substitutional to the total implanted O) of about 5%, similar to what we observed in the case of the N-ion implantation synthesized  $\text{GaN}_x\text{As}_{1-x}$ . [16, 17]. The results are also consistent with the low solubility of O in II-VI alloys. In fact, in most bulk grown II-VI compounds, an upper limit of  $\sim 10^{17} \text{ cm}^{-3}$  of O can be incorporated [18].

Fig. 2 shows a series of PR spectra from seven  $\text{Cd}_{1-y}\text{Mn}_y\text{O}_x\text{Te}_{1-y}$  alloys formed by high dose O (5.4%) implantation (after RTA at 600 – 700°C depending on  $y$ ) and their corresponding unimplanted  $\text{Cd}_{1-y}\text{Mn}_y\text{Te}$  crystals for a wide range of MnTe mole fraction,  $0.2 < y < 0.64$ . Significant band gap reductions can be observed in all of the  $\text{O}^+$ -implanted  $\text{Cd}_{1-y}\text{Mn}_y\text{Te}$  crystals, indicating the formation of  $\text{Cd}_{1-y}\text{Mn}_y\text{O}_x\text{Te}_{1-y}$  alloys throughout the range of Mn content studied. We note that there is a significant increase

of the band gap reduction and an associated increase of the line broadening for the Mn alloy compositions larger than about 60%.

The measured band gap energies for samples in Fig. 2 are displayed in Fig. 3 together with the known dependencies of the conduction band minima and our estimate of  $E_O$  as a function of  $y$ . Assuming that  $C_{OM}$  is independent of  $y$  a best fit of the measured band gap energies of the O ion synthesized  $Cd_{1-y}Mn_yO_xTe_{1-x}$  alloys using the BAC model [Eq. (1)] for  $y < 0.55$  yields a  $C_{OM}^2 x$  value of 0.02. As is seen in Fig. 3 the  $E_O$  level falls below  $E_M$  for  $y > 0.55$ . This corresponds to a change in the nature of the lowest CB minimum from delocalized, band-like for  $y < 0.55$  to localized oxygen like at  $y > 0.55$ . This transition is most likely responsible for the large increase of the PR line width observed in the samples with  $y > 0.6$ .

The results of this study demonstrate the existence of a new, broad class of group II-O<sub>x</sub>-VI<sub>1-x</sub> alloys with properties analogous to the extensively studied and practically very important III-N<sub>x</sub>-V<sub>1-x</sub> materials. It is anticipated that, similar to III-N<sub>x</sub>-V<sub>1-x</sub> materials, these new alloys should exhibit novel properties and expand the range of possible applications of group II-VI materials. For example, by adjusting the energy gap using the O content in these alloys one can make a variable gap semiconductor that is lattice matched to a specific substrate. Moreover, since the incorporation of O into II-VI alloys results in a downward shift of the conduction band edge it is expected that II-O<sub>x</sub>-VI<sub>1-x</sub> alloys should exhibit much enhanced activation efficiency for shallow donors, similar to the case in group III-N<sub>x</sub>-V<sub>1-x</sub> alloys [19-21]. In particular it is expected that the elusive n-type ZnTe could be realized by the formation of ZnO<sub>x</sub>Te<sub>1-x</sub> with small O content.

In conclusion, we have successfully synthesized the  $Cd_{1-y}Mn_yO_xTe_{1-y}$  highly mismatched alloys by O implantation in  $Cd_{1-y}Mn_yTe$  crystals. The O-induced reduction of the fundamental band gap is well described by the anticrossing interaction between the localized states of O and the extended states of the conduction band of the matrix II-VI

crystal. The results demonstrate an existence of a new broad class of highly mismatched group II-O<sub>x</sub>-VI<sub>1-x</sub> semiconductor alloys.

This work was supported by the "Photovoltaic Materials Focus Area" in the DOE Center of Excellence for the Synthesis and Processing of Advanced Materials, Office of Science, Office of Basic Energy Sciences, Division of Materials Sciences under U.S. Department of Energy Contract No. DE-ACO3-76SF00098. The work at Purdue received support from National Science Foundation grant No. DMR 98-00858 and from Purdue University through the University Reinvestment Program.



## REFERENCES

1. M. Weyers, M. Sato and H. Ando, *Jpn. J. Appl. Phys.* **31**, L853 (1992).
2. M. Kondow, K. Uomi, K. Hosomi, and T. Mozume, *Jpn. J. Appl. Phys.* **33**, L1056 (1994).
3. W. G. Bi and C. W. Tu, *J. Appl. Phys.* **80**, 1934 (1996).
4. K. Uesugi, N. Morooka, and I. Suemune, *Appl. Phys. Lett.* **74**, 1254(1999).
5. J. F. Geisz, D. J. Friedman, J. M. Olson, S. R. Kurtz, and B. M. Keyes, *J. Cryst. Growth* **195**, 401 (1998).
6. W. Shan, W. Walukiewicz, K. M. Yu, J. Wu, J. W. Ager, E. E. Haller, H. P. Xin, and C. W. Tu, *Appl. Phys. Lett.* **76**, 3251 (2000).
7. K. M. Yu, W. Walukiewicz, W. Shan, J. Wu, J. W. Ager III, E. E. Haller, H. P. Xin, and C. W. Tu, *Appl. Phys. Lett.* **78**, 1077 (2001).
8. W. Shan, W. Walukiewicz, J. W. Ager III, E. E. Haller, J. F. Geisz, D. J. Friedman, J. M. Olson, and S. R. Kurtz, *Phys. Rev. Lett.* **82**, 1221(1999).
9. W. Walukiewicz, W. Shan, J. W. Ager III, D. R. Chamberlin, E. E. Haller, J. F. Geisz, D. J. Friedman, J. M. Olson, and S. R. Kurtz, in *Photovoltaics for the 21<sup>st</sup> Century*, edited by V. K. Kapur, R. D. McDonnell, D. Carlson, G. P. Ceasar, A. Rohatgi (Electrochemical Society Press, Pennington, 1999) p. 190.
10. C. Skierbiszewski, P. Perlin, P. Wiśniewski, W. Knap, T. Suski, W. Walukiewicz, W. Shan, K. M. Yu, J.W. Ager, E.E. Haller, J.F. Geisz, and J.M. Olson, *Appl. Phys. Lett.* **76**, 2409 (2000).
11. W. Walukiewicz, W. Shan, K. M. Yu, J. W. Ager III, E. E. Haller, I. Miotkowski, M. J. Seong, H. Alawadhi, and A. K. Ramdas, *Phys. Rev. Lett.* **85**, 1552 (2000).
12. M. J. Seong, H. Alawadhi, I. Miotkowski, A. K. Ramdas, and, S. Miotkowska, *Phys. Rev.* **B62**, 1866 (2000).
13. D. E. Aspnes, *Surf. Sci.* **37**, 418 (1973).

14. The damage profiles in  $\text{Cd}_{1-y}\text{Mn}_y\text{Te}$  crystals created by Ne, Cl and O ions were calculated by the TRIM software package.
15. M. J. Seong, H. Alawadhi, I. Miotkowski, A. K. Ramdas and S. Miotkowska, *Phys. Rev. B* **60**, R16275(1999).
16. W. Shan, K. M. Yu, W. Walukiewicz, J. W. Ager, E. E. Haller and M. C. Ridgway, *Appl. Phys. Lett.* **75**, 1410 (1999).
17. K. M. Yu, W. Walukiewicz, J. Wu,, J. W. Beeman, J. W. Ager III, E. E. Haller, W. Shan, X. P. Xin, C. W. Tu, and M. C. Ridgway, *J. Appl. Phys.* **90**, 2227 (2001).
18. M. J. Seong, I. Miotkowski, and A. K. Ramdas, *Phys. Rev.* **B58**, 7734 (1998).
19. K. M. Yu, W. Walukiewicz, W. Shan, J. W. Ager III, J. Wu, E. E. Haller, J. F. Geisz, D. J. Friedman, J. M. Olson, and Sarah R. Kurtz, *Phys. Rev.* **B61**, R13337 (2000).
20. K. M. Yu, W. Walukiewicz, W. Shan, J. Wu, J. W. Ager III, E. E. Haller, J. F. Geisz, and M.C. Ridgway, *Appl. Phys. Lett.* **77**, 2858 (2000).
21. K. M. Yu, W. Walukiewicz, W. Shan, J. Wu, J. W. Ager III, and E. E. Haller, *Appl. Phys. Lett.* **77**, 3607 (2000).

## FIGURE CAPTIONS

- Figure 1 Photomodulated reflectance (PR) spectra of three low dose ( $y=0.017, 0.043, 0.19$ ) and a high dose ( $y=0.19$ ) O-implanted  $\text{Cd}_{1-y}\text{Mn}_y\text{Te}$  samples after rapid thermal annealing (RTA) at  $600^\circ\text{C}$  (O imp.;  $600^\circ\text{C}$ ). PR spectra from the corresponding unimplanted  $\text{Cd}_{1-y}\text{Mn}_y\text{Te}$  crystals are also shown for direct comparison.
- Figure 2 A series of PR spectra of seven  $\text{Cd}_{1-y}\text{Mn}_y\text{O}_x\text{Te}_{1-y}$  quaternaries for a wide range of MnTe mole fraction,  $0.2 < y < 0.64$  formed by high dose O (5.7%) implantation and their corresponding unimplanted  $\text{Cd}_{1-y}\text{Mn}_y\text{Te}$  crystals.
- Figure 3. The room temperature band gap energies of the unimplanted and O implanted  $\text{Cd}_{1-y}\text{Mn}_y\text{Te}$  samples as a function of  $y$  for  $0.1 < y < 0.64$ . The known dependencies of the conduction band minima on the MnTe mole fraction and our estimate of  $E_O$  on  $y$  are also shown. The solid lines are the upper and lower subbands calculated by the BAC model using a  $C_{OM}^2x$  value of 0.02.

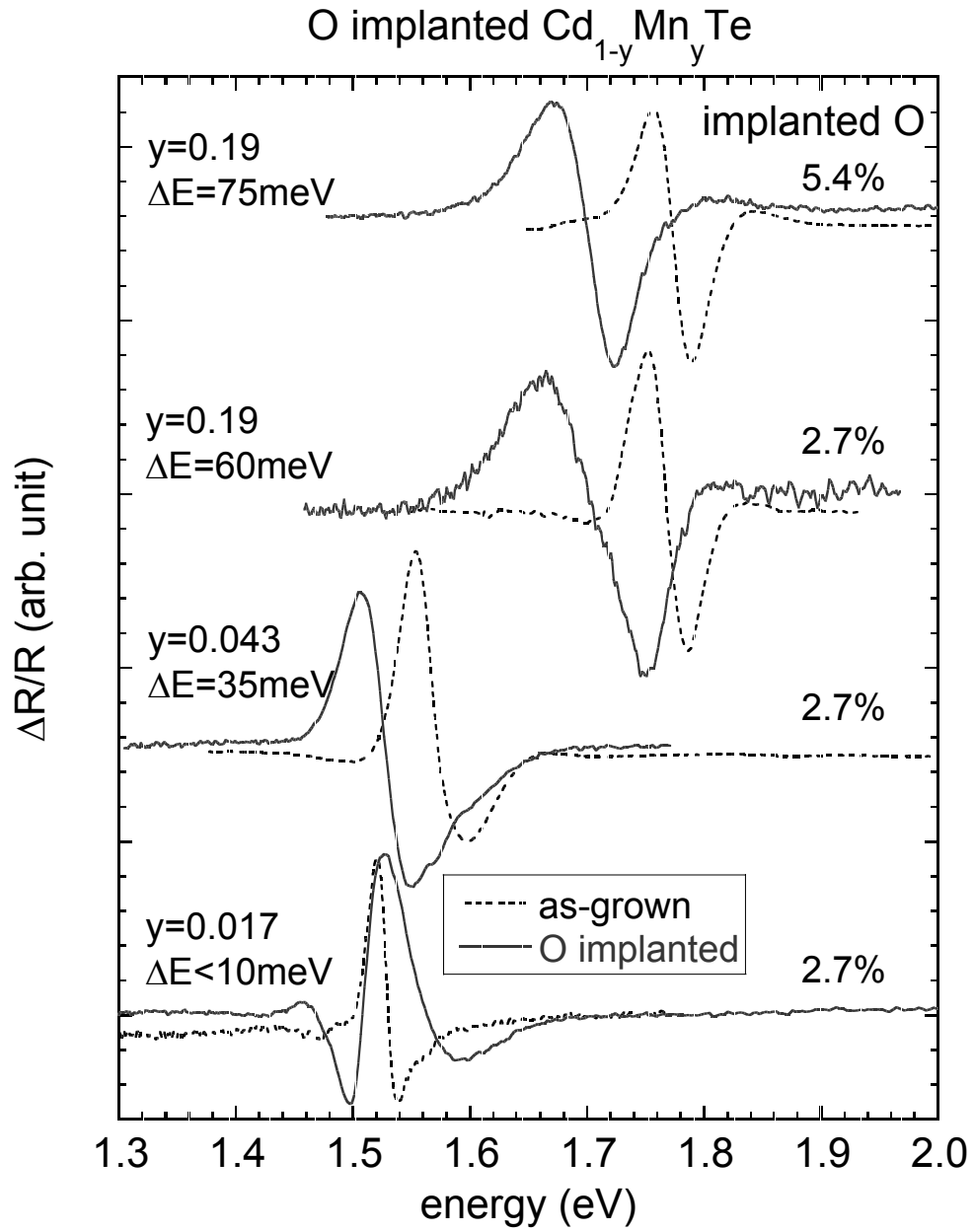


Fig. 1

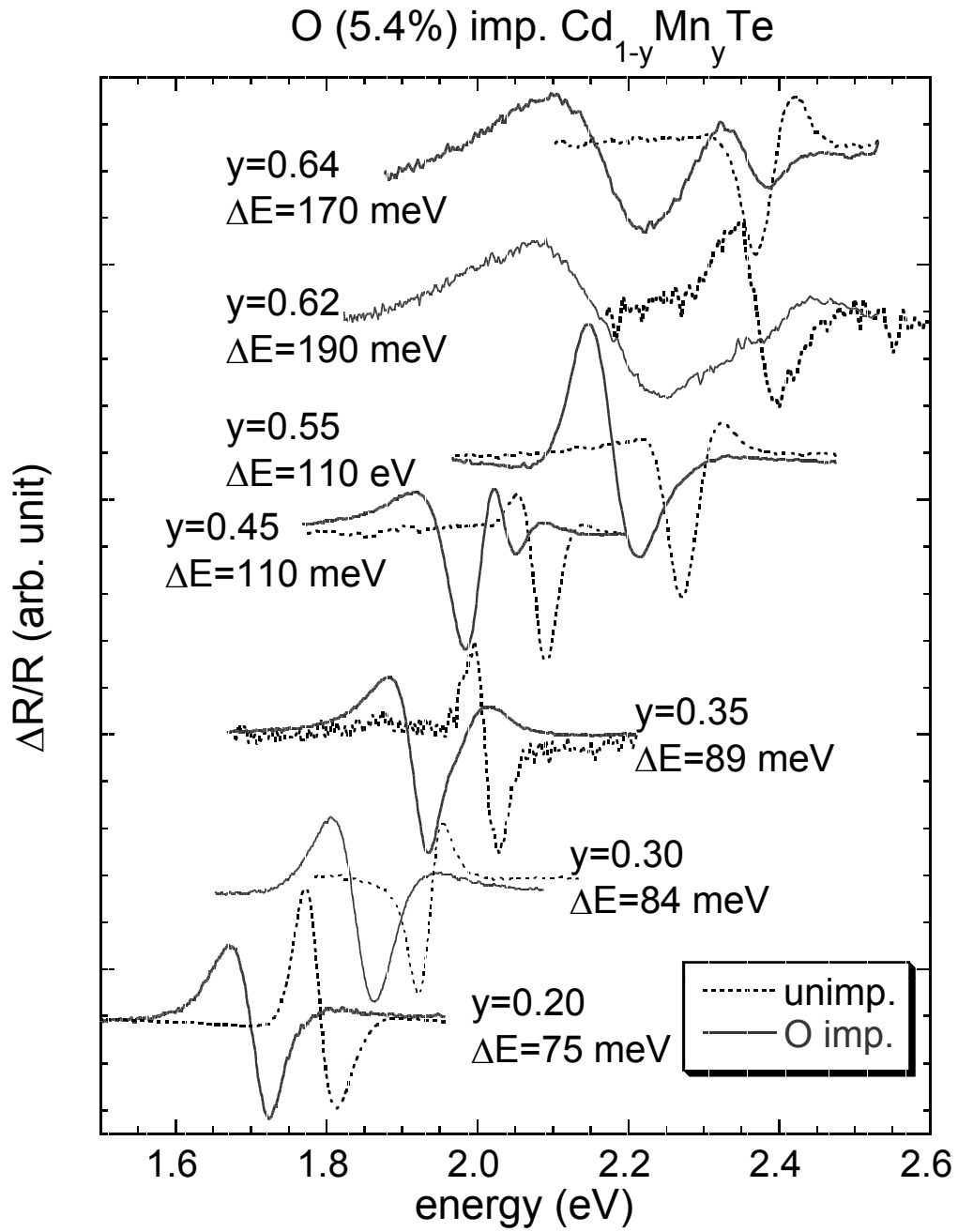


Fig. 2

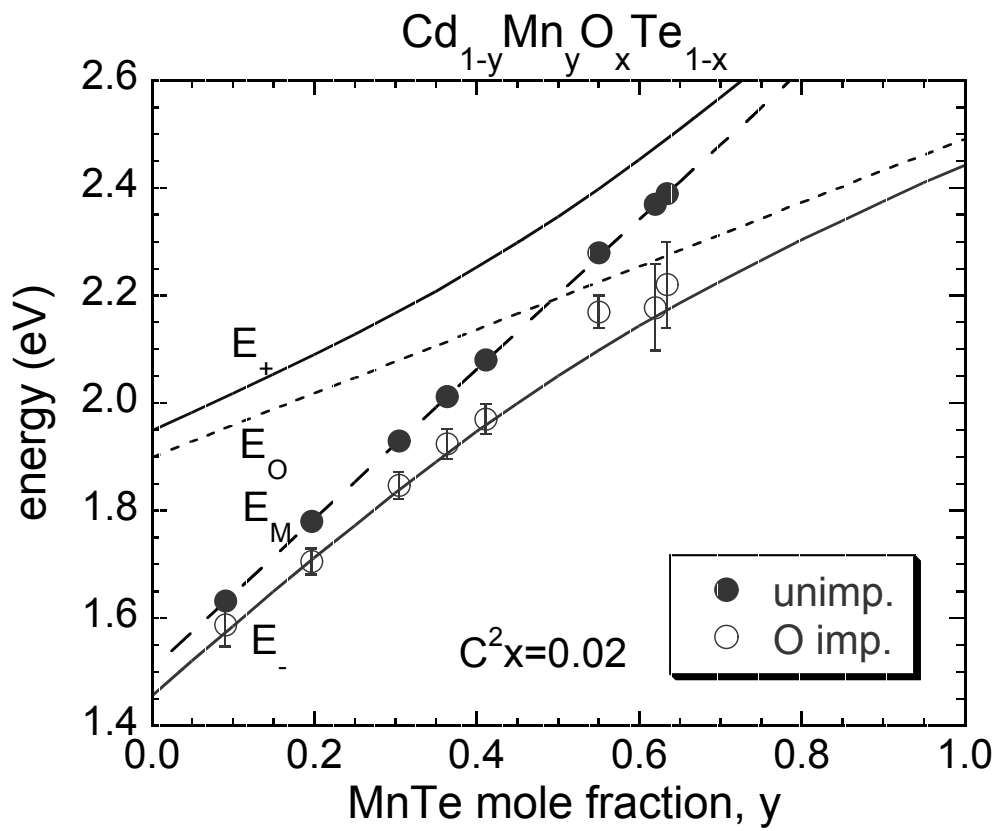


Fig. 3